ОБЪЕДИНЕННЫЙ
ИНСТИТУТ
ЯДЕРНЫХ
ИССЛЕДОВАНИЙ

Дубна

E1-2000-308

V.P.Bamblevski, A.R.Krylov, A.Polanski,
G.N.Timoshenko, V.N.Shvetzov

THE INVESTIGATION OF THE RADIATION FIELD AROUND THE THICK LEAD TARGET IRRADIATED BY THE 650 MeV PROTONS

Part 2. The Measurements of the Angular and Spatial Distributions of the Hadron's Yield from the Target

Submitted to «Nuclear Instruments and Methods A»

2000

The present part of the paper is dedicated to the activation detector technique used in the experiment for the investigation of the angular distributions of secondary hadrons around the target, measuring of the longitudinal distribution of the secondaries along the target and the estimation of the total yield of the secondaries from the target. The general description of the experimental arrangement and conditions is given in Part 1of the present paper.

ANGULAR DISTRIBUTIONS OF THE HADRONS AROUND THE TARGET

For the investigation of the hadron yield from the target the activation detectors (AD) from ^{12}C and ^{27}Al were used. The carbon-contained detector was a polyester disk with 6 cm in diameter and 1 cm thickness. The aluminium detector represented the batch of the foils with dimension of 6×6 cm^2 and total thickness of 0.1 cm. The arrangement of the AD is shown in Fig. 4 of Part 1. The detectors were placed at distance of 1 meter around the target center in the horizontal plane from 0^0 up to 165^0 via every 15^0 relative to the beam direction. The detectors were irradiated by secondary hadrons (neutrons, protons and π-mesons) from the target at the high intensity of the proton beam.

The activities of the ^{18}F, ^{11}C and ^{24}Na ($^{27}Al(h,x)^{18}F$, $^{12}C(h,x)^{11}C$ and $^{27}Al(h,x)^{24}Na$ reactions) with the thresholds of 40, 20 and 6 MeV accordingly) were then measured by the low-background gamma spectrometer. The AD processing runs were started as soon as possible after their irradiation. The detector's activities were measured by two low background spectrometers (single NaI(Tl) gamma-spectrometer and gamma-gamma coincidence NaI(Tl) spectrometer with good calibrated effectivities).

The flux of the charged particles from the target was slight in comparison with the neutron flux, and the neutrons produced the main contribution to the AD activities. However, the interpretation of the AD activities in the neutron flux term only would be a rough enough approximation due to the greater activation cross-section value for charged particles and strong dependence of these cross-sections on these particles' energy. That is why the results of the measurements are given in the term of specific activity: $A^{\infty}/(M_d \cdot I)$, where A^{∞} is detector's activity extrapolated to the infinite time of irradiation (Bk), M_d is the total amount of ^{12}C atoms in the detector and I is the average beam proton intensity during the irradiation time (proton·s^{-1}). This value is equivalent of the reaction rate. The experimental verification of the calculation of the internuclear cascade into the target can be performed by means of the calculation of these specific detector's activities induced by the secondaries as well.

The angular distributions of the ^{18}F, ^{11}C and ^{24}Na specific activities are shown in Fig. 1. The double symbols in the curves are the date from the two gamma spectrometers. Because of the big length of the target the distributions of ^{18}F and ^{11}C have the apparent maximum at about 15^0. The main part of the nuclear interactions takes place in the initial part of the target (see it below) and the target length for the neutrons generated there under small angles to the beam direction is larger than in the side direction. The angular resolution was insufficient for the definition of the exact maximum positions for the ^{18}F and ^{11}C distributions. In reality their positions can be found obviously in the angular range $10^0 \div 20^0$ and its place can depends on the energy threshold of the detector. In this picture the graphit data (renormalized) from the multisphere spectrometer measurements are presented also as the big square symbols. For ^{24}Na distribution the extented maximum is observed in the angle interval $40^0 \div 80^0$. The degradation rate of the activities also depends on the energy threshold of the reactions. At the threshold of 6 MeV (^{24}Na) the angular distribution drops slightly in the wide-angle range. In Fig. 1 the ^{24}Na data for the energy range from 6 to 20 MeV are shown too as the short dashed curve. These data were obtained, as the first approach, with the approximation of the ^{27}Al(h,x)^{24}Na reaction cross-section above 20

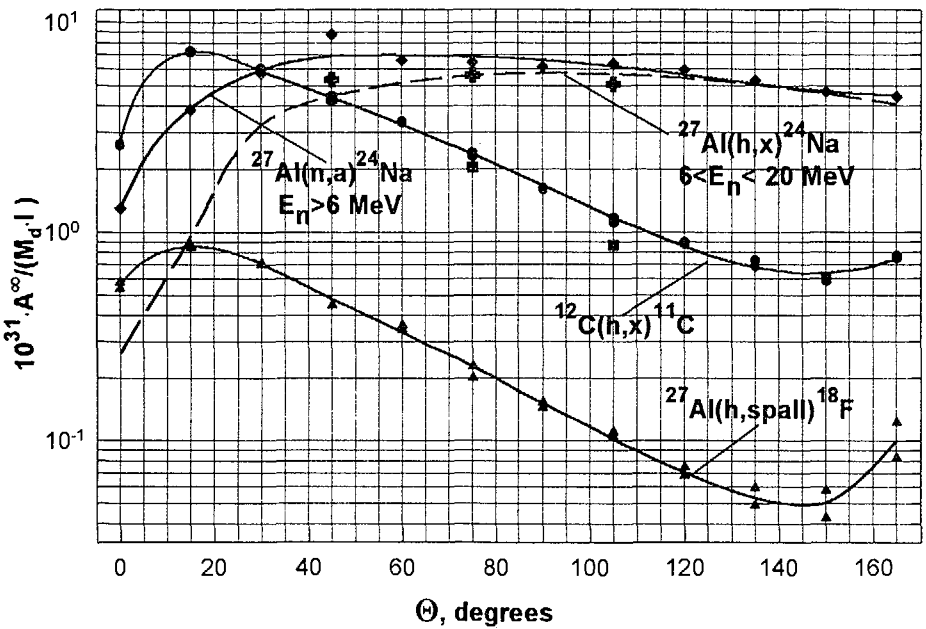

Fig.1. The angular distributions of the specific activities of the ^{12}C and ^{27}Al activation detectors spaced around the target.

MeV by the constant similar the $^{12}C(h,x)^{11}C$ reaction. In this case the angular distribution becomes practically flat at angles more than 40^0.

The background subtraction in these measurements was not carried out because of the short distance between the AD and the target and owing to the high energy detector's threshold (the largest parts of the SB background neutron spectrum are under the thresholds (see Fig.7 of Part 1). In accordance with the estimations based on this spectrum the background AD activities were less than 6% for ^{24}Na, 0,6% for ^{11}C and 0,1% for ^{18}F.

The errors of the specific activities are mainly the gamma-spectrometers calibration errors, the statistic errors of the apparatus spectra, the proton beam monitoring errors and the accuracy of the correction calculation for ^{24}Na decay at the ^{18}F measurement. In general, the total errors of the measurements were in the limits from ~ 6% in maximums of the distributions to 15% in the minimums of the distributions.

THE SPATIAL DISTRIBUTIONS OF THE HADRONS AROUND THE TARGET

For the longitudinal distribution of the hadron yield measuring, the target was wrapped round the layers of the aluminium foil and the polyethylene film. The disks from such layers of the AD were mounted on the front and rear surfaces of the target. After irradiation the longitudinal detectors were cross-cuted on eight equal parts and theirs activities were measured then separately. The beam protons produced the activation of the front detectors as well as the secondaries from the target. In order to subtract the AD activities due to the initial protons the same detectors were placed at distance 30 cm from the target up-stream of the beam. The activation cross-section was taken as 30.5 /1/ and 11.2 /2/ mb for the $^{12}C(p,np)^{11}C$ and $^{27}Al(p,x)^{24}Na$ reactions accordingly. The arrangement of the AD around the target is shown in Fig. 2.

The results of the measurements of the longitudinal specific activity distributions are presented in Fig 3. The reactions $^{12}C(h,x)^{11}C$,

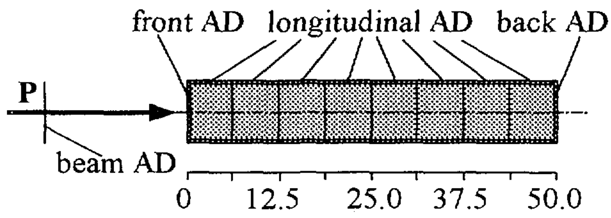

Fig.2. The arrangement of the activation detectors around the target.

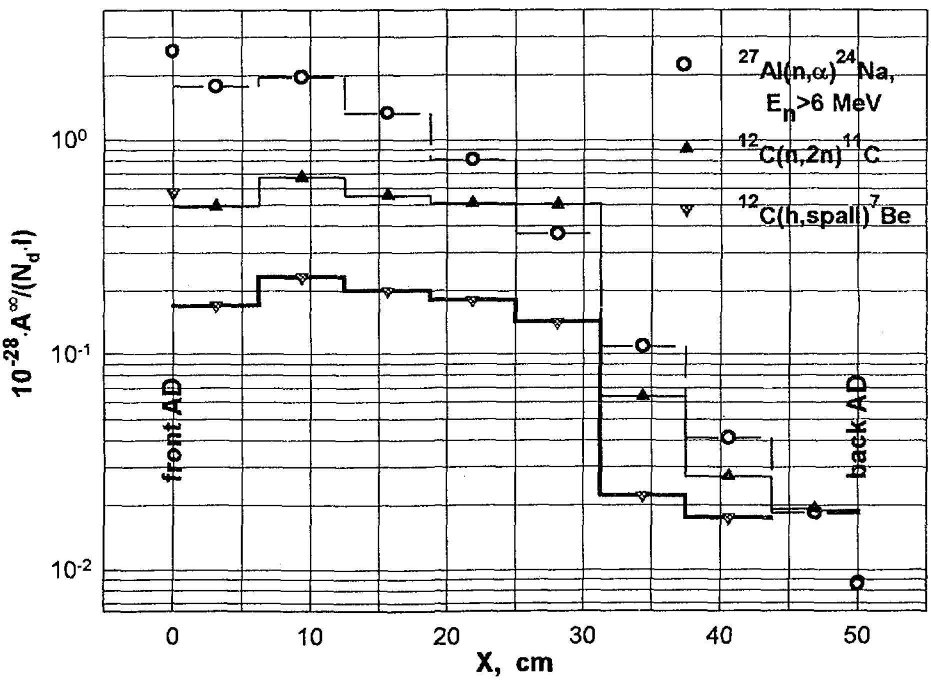

Fig.3 The spatial distribution of the detector specific activities on the target surface.

$^{27}Al(h,x)^{24}Na$ and $^{12}C(h,spall)^{7}Be$ with energy threshold ~ 30 MeV are used. The experimental data are presented in the same terms as the angular activities distributions. There are given also (separately) the values for the front (at 0 cm) and rear (at 50 cm) surfaces of the target. The very fast drop of the longitudinal distributions for ^{24}Na is evidence of generation of the overwhelming majority of neutrons in the initial part of the target. It was confirmed by the measurements with the gamma dosimeter of the prompt gamma radiation levels from the different parts of the target just after the experimental run. The induced radiation levels are differed approximately in three decades close by the initial and the terminal parts of the target. The longitudinal distributions for ^{11}C and ^{7}Be isotopes have more flat initial parts. Obviously, it is owing to the growth of the neutron relaxation length with the neutron energy.

The total specific activities of the whole surface of the AD (induced by the hadrons escaped from the target in 4π sr) were defined from these measurements as following:

$$A_t = (A_f^\infty \cdot S_f / M_{df} \cdot I + \sum_{i=1}^{8} A_{li}^\infty \cdot S_{li} / M_{di} \cdot I + A_b^\infty \cdot S_b / M_{db} \cdot I) / S$$

where $A_f^\infty / M_{df} \cdot I$ and $A_b / M_{db} \cdot I$ - the specific activities of the front and back AD accordingly; $A_{li}^\infty / M_{di} \cdot I$ the scecific activity of the *i*-longitudinal AD; S_f, S_b and S_{li} - the squares of the front, back and longitudinal AD; S – the total square of the AD (1458 cm^2). The value of the $A_t \cdot S$ is convenient for the rough estimation of the total neutron yield from the target. In the first approximation, the "effective" ^{11}C reaction cross-section σ_{ef} (taking into account the admixture of the charged particles) can be taken as 23.5 mb for the whole energy range. In this case the yield of the neutron with energies more than 20 founds as $A_t \cdot S / \sigma_{ef}$. The specific activities of the whole AD surface and the estimations of the neutron yields are presented in Table 1. The total errors of these data are estimated in limits of 8%.

Table 1.

Isotope	E_n, MeV	A_t	Neutron yield per 1 proton (E_n > 20 MeV)
^{24}Na	> 6	$8{,}14\cdot10^{-29}$	—
^{11}C	> 20	$3.22\cdot10^{-29}$	2

On the basis of the obtained data about the angle distributions of the hadrons the total specific activities around the target were estimated too by using the data interpolation and by the following angular integration in the 4π sr solid angle. These values are conformed with the data of the spatial distributions.

CONCLUSION

The obtained neutron spectra in the fixed points of radiation field around the target have a reasonable agreement with the results of the measuring (with the activation technique) of the angle distribution of the hadrons escaped from the target. In Fig. 1 the total neutron fluences under 45^0, 75^0 and 105^0 measured by the SB technique (without energy threshold) are shown in arbitrary units (big cross symbols) in comparison with the ^{24}Na (6< E_n.20 MeV) data. In this angle range the neutron (hadron) yield from the target is practically constant and most parts of the neutron spectra are similar too. The differences are observed in the high-energy part of the spectra where the errors become significant. As it was pointed earlier, the multisphere technique has poor information in this energy range. Because it is expedient to use the other spectrometric methods for the separate measuring of the high-energy parts of the neutron spectra. It can be the time-of-flight method or the proton recoil method especially designed for the given experimental conditions.

As far as the activation technique it is expedient to extend the energy range of the measurements by use of $^{32}S(n,p)^{32}P$ reaction with the threshold about 3 MeV and ^{209}Bi(n,f) reaction with the threshold about 50 MeV in combination with the nuclear track detectors.

ACKNOWLEDGEMENT

We are very grateful to Drs. P. Shishlyanikov, A.Molokanov, I. Mirochin, S. Gustov for excellent beam focusing and regulation during the experiment and to Prof. A.Sissakian, I.Puzynin and V.Barashenkov for the permanent support of this work.

This work was carried out by the partial financial support of the Forschungszentrum Karlsruhe, contract № 315/20171212/IKET

REFERENCES

1. J.B.Cumming. Ann. Rev. Nucl. Sci. 13, 1963, p.261
2. R.Michel et al. Nucl. Instr. and Meth. B, 103, 1995, p.183;
   Th.Schiekel et al. Nucl. Instr. and Meth. B, 114, 1996, p. 91.

Received by Publishing Department
on December 21, 2000.